The Modeling and Simulation of an Autonomous Quad-Rotor Microcopter in a Virtual Outdoor Scenario

Aleksandar Rodić[1], Gyula Mester[2]

[1] University of Belgrade, Institute Mihajlo Pupin, Robotics Laboratory, Belgrade, Serbia, aleksandar.rodic@pupin.rs

[2] University of Szeged, Institute of Informatics, Department of Technical Informatics, Robotics Laboratory, Szeged. Hungary, gmester@inf.u-szeged.hu

Abstract: This paper presents the modeling and simulation of an autonomous quad-rotor microcopter in a virtual outdoor scenario. The main contribution of this paper focuses on the development of a flight simulator to provide an advanced R/D tool suitable for control design and model evaluation of a quad-rotor systems to be used for control algorithm development and verification, before working with a real experimental system. The main aspects of modeling of rotorcraft kinematics and rigid body dynamics, spatial system localization and navigation in a virtual outdoor scenario are considered in the paper. Some high-level control aspects are considered, as well. Finally, several basic maneuvers (examples) are investigated and simulated in the paper to verify the simulation software capabilities and engineering capabilities.

Keywords: modeling; simulation; autonomous quad-rotor microcopter; Xaircraft X 650; rotorcraft; virtual outdoor scenario; quad-rotor dynamics; spatial navigation; GPS coordinates; GPS navigation, simulation example

1 Introduction

Over the past several decades, a growing interest has been shown in robotics. In fact, several industries (automotive, medical, manufacturing, space, . . .) require robots to replace men in dangerous, boring or onerous situations. A wide area of this research is dedicated to aerial platforms. Several structures and configurations have been developed to allow 3D movements [1]-[11]. For example, there are blimps, fixed-wing planes, single rotor helicopters, bird-like prototypes, quad-rotors, etc. Each of these has advantages and drawbacks. The vertical take-off and landing requirements exclude some of the aforementioned configurations. However, the platforms which show these characteristics have a unique ability for vertical, stationary and low speed flight.

The quad-rotor architecture has been chosen for this research for its low dimension, good maneuverability, simple mechanics and payload capability. As the main drawback, the high energy consumption can be mentioned. However, the trade-off results are very positive. This structure can be attractive in several applications, in particular for surveillance, for imaging dangerous environments, and for outdoor navigation and mapping (Fig. 1).

Figure 1
Quad-rotor XAircraft X650

The study of the kinematics and dynamics helps to understand the physics of the quad-rotor and its behavior [1], [2]. Together with modeling, the determination of the control algorithm structure is very important for improving stabilization. The whole system can be tested thanks to a Matlab-Simulink program that is interfaced with the remote controller. This software provides a 3D graphic output as well as status data for debugging the system performance. The real platform is developed by creating a system (integration) of interconnected devices. Two types of sensors are used for measuring the robot attitude and for measuring its height from the ground. For the first, an Inertial Measurement Unit (IMU) was adopted, while the distance was estimated with a SOund Navigation And Ranging (SONAR) and an InfraRed (IR) modules. The data processing and the control algorithm are handled in the Micro Control Unit (MCU) which provides the signals to the motors. Actually, four motor driver boards are needed to amplify the power delivered to the motors. Their rotation is transmitted to the propellers which move the entire structure (see Fig. 1).

The paper is organized as follows: Section 1: Introduction. In Section 2, the modeling of the Quad-rotor aircraft and the control strategy are presented. In Section 3, the GPS navigation of the Quad-rotor is illustrated. In Section 4, the simulation results are illustrated. Conclusions are given in Section 5.

2 Modeling of the Quad-Rotor Aircraft

Rotary wing aerial vehicles have distinct advantages over conventional fixed wing aircrafts in surveillance and inspection tasks because they can take-off and land in limited spaces and easily fly above the target. A quad-rotor is a four rotor helicopter. An example of one is shown in Fig. 1. Helicopters are dynamically unstable and therefore suitable control methods are needed to make them stable. Although unstable dynamics is not desirable, it is good from the point of view of agility. The instability comes from changes in the helicopter parameters and from disturbances such as a wind gust or air density variation. A quad-rotor helicopter is controlled by varying the rotor speed, thereby changing the lift forces [1], [2]. It is an under-actuated dynamic vehicle with four input forces and six outputs coordinates. One of the advantages of using a multi-rotor helicopter is the increased payload capacity. Quad-rotors are highly maneuverable, which allows for vertical take-off/landing, as well as flying into hard-to-reach areas; but the disadvantages are the increased helicopter weight and increased energy consumption due to the extra motors. Since the machine is controlled via rotor-speed changes, it is more suitable to utilize electric motors. Large helicopter engines, which have a slow response, may not be satisfactory without incorporating a proper gear-box system.

Unlike typical helicopter models (and regular helicopters), which have variable pitch angles, a quad-rotor has fixed pitch angle rotors, and the rotor speeds are controlled in order to produce the desired lift forces. The basic motions of a quad rotor can be described using the model presented in Figs. 2 and 3.

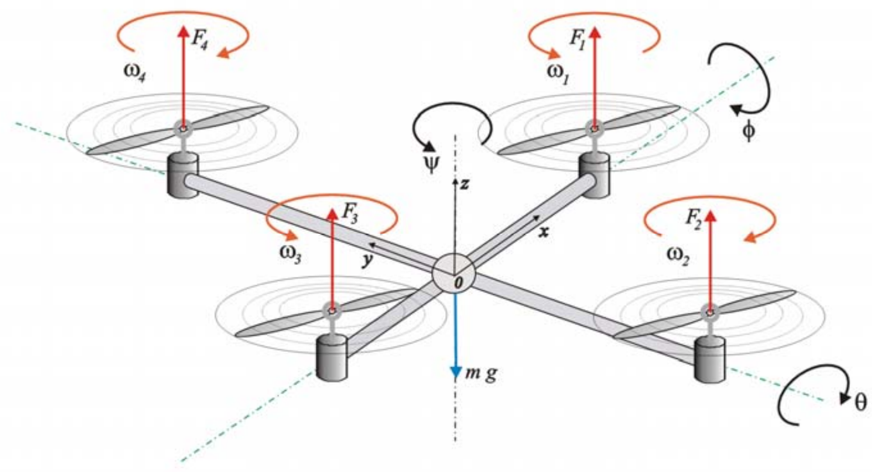

Figure 2

3 D motion, commonly used model of the quad-rotor

In the first method, the vertical motion of the helicopter can be achieved by changing all of the rotor speeds at the same time. Motion along the x-axis (Fig. 2) is related to tilt around the y-axis. This tilt can be obtained by decreasing the speed of propeller 1 and increasing corresponding speed of propeller 2. This tilt also produces acceleration along the x-axis. Similarly, y-motion is the result of the tilt around the x-axis. A good controller should be able to reach a desired yaw angle while keeping the tilt angles and the height constant.

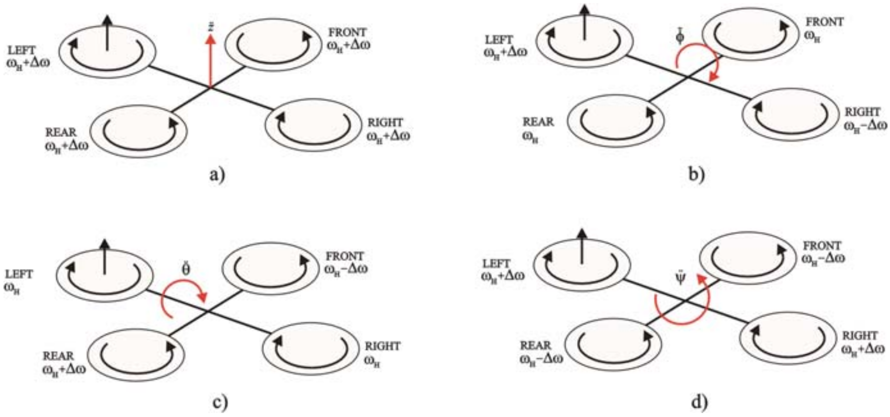

Figure 3
Definition of a) throttle, b) roll, c) pitch and d) yaw movements

2.1 Analysis of Possible Movements

The quad-rotor is satisfactorily modeled with four rotors in a cross configuration (Fig. 1). This cross structure is quite thin and light; however, it shows robustness via mechanically linking the motors (which are heavier than the structure). Each propeller is connected to the motor through the reduction gears. All the propellers have fixed and parallel axes of rotation. Furthermore, they have fixed-pitch blades and their air flows points downwards (to get an upward lift). These considerations point out that the structure is quite rigid, and the only things that can be varied are the propeller speeds. In this section, neither the motors nor the reduction gears are important to consider because the movements are directly related only to the propeller-velocities. Another neglected component is the electronic box. As in the previous instance, the electronic box is not important for understanding how the quad-rotor flies. It thus follows that the basic model for evaluating the movements of a quad-rotor is composed only of a thin cross structure with four propellers on the ends. The front and the rear propellers rotate counter-clockwise, while the left and the right ones turn clockwise. This configuration of pairs moving in opposite directions removes the need for a tail rotor (which is needed in the standard helicopter structure). Fig. 1 shows the structure model in hovering condition where all the propellers have the same speed $\omega_i = \omega_H$, $i = 1,...,4$. In Fig. 2 all the propellers rotate at the same (hovering) speed ω_H (rad/s) to counterbalance the acceleration due to gravity. Thus, the quad-rotor performs stationary flight and no forces or torques move it from its position. Even though, the quad-rotor has 6 DOFs, it is equipped just with four propellers, hence it is not possible to reach a desired set-point for all the DOFs, but at maximum four. However, thanks to its structure, it is quite easy to choose the four best controllable variables and to decouple them to make the control task easier. The four quad-rotor targets are thus related to the four basic movements which allow the helicopter to reach a certain height and attitude. The description of these basic movements follows [3]:

2.1.1 The Throttle Movements

This command is provided by increasing (or decreasing) all the propeller speeds by the same amount. It leads to a vertical force with respect to body-fixed frame which raises or lowers the quad-rotor. If the helicopter is in a horizontal position, the vertical direction of the inertial frame and that one of the body-fixed frame coincide. Otherwise the provided thrust generates both vertical and horizontal accelerations in the inertial frame. Fig. 3a shows the throttle command in the quad-rotor sketch. The speed of the propellers ω_i, $i = 1,...,4$ in this case are equal to $\omega_H + \Delta\omega$ for each. The $\Delta\omega$ (rad/s) is a positive variable which represents an increment with respect to the constant value. The $\Delta\omega$ must not be too large because the model would eventually be influenced by strong non-linearities or saturations.

2.1.2 The Roll Movements

This command is provided by increasing (or decreasing) the speed of the left propeller and by decreasing (or increasing) the speed of the right one. This leads to torque with respect to the $x-$ axis (Fig. 2), which makes the quad-rotor turn. The overall vertical thrust is the same as in hovering, hence this command leads only to a roll angle acceleration (in the first approximation). Figure 3b shows the roll command on a quad-rotor sketch. The positive variable $\Delta\omega$ is chosen to maintain the vertical thrust unchanged. As in the previous case, they must not be too large because the model would eventually be influenced by strong non-linearities or saturations.

2.1.3 The Pitch Movements

This command is very similar to the roll and is provided by increasing (or decreasing) the speed of the rear propeller and by decreasing (or increasing) the speed of the front one. This leads to torque with respect to the $y-$ axis which makes the quad-rotor turn. The overall vertical thrust is the same as in hovering, hence this command leads only to a pitch angle acceleration (in the first approximation). Figure 3c shows the pitch command on a quad-rotor sketch. As in the previous case, the positive variable $\Delta\omega$ is chosen to maintain the vertical thrust unchanged, and it cannot be too large.

2.1.4 The Yaw Movements

This command is provided by increasing (or decreasing) the front and rear propellers' speed and by decreasing (or increasing) that of the left-right couple. It leads to torque with respect to the $z-$ axis which makes the quad-rotor turn. The yaw movement is generated thanks to the fact that the left-right propellers rotate clockwise while the front-rear ones rotate counter-clockwise (Fig. 3d). Hence, when the overall torque is unbalanced, the helicopter turns on itself around z. The total vertical thrust is the same as in hovering, hence this command leads only to a yaw angle acceleration (in the first approximation). Figure 3d shows the yaw command on a quad-rotor sketch.

2.2 The Newton-Euler Model

To describe the motion of a 6 DOF rigid body it is usual to define two reference frames (Fig. 4):

- the earth inertial frame (E-frame), and
- the body-fixed frame (B-frame)

The equations of motion are more conveniently formulated in the B-frame because of the following reasons:

- The inertia matrix is time-invariant.
- Advantage of body symmetry can be taken to simplify the equations.
- Measurements taken on-board are easily converted to body-fixed frame.
- Control forces are almost always given in body-fixed frame.

The E-frame (*OXYZ*) is chosen as the inertial right-hand reference. *Y* points toward the North, *X* points toward the East, *Z* points upwards with respect to the Earth, and *O* is the axis origin. This frame is used to define the linear position (in meters) and the angular position (in radians) of the quad-rotor. The B-frame (*oxyz*) is attached to the body. *x* points toward the quad-rotor front, *y* points toward the quad-rotor left, *z* points upwards and o is the axis origin. The origin *o* is chosen to coincide with the center of the quad-rotor cross structure. This reference is right-hand, too. The linear velocity v (m/s), the angular velocity Ω (rad/s), the forces *F* (N) and the torques *T* (Nm) are defined in this frame. The linear position of the helicopter (*X, Y, Z*) is determined by the coordinates of the vector between the origin of the B-frame and the origin of the E-frame according to the equation. The angular position (or attitude) of the helicopter (ϕ, θ, ψ) is defined by the orientation of the B-frame with respect to the E-frame. This is given by three consecutive rotations about the main axes which take the E-frame into the B-frame. In this paper, the “roll-pitch-yaw” set of Euler angles were used. The vector that describes the quad-rotor position and orientation with respect to the E-frame can be written in the form:

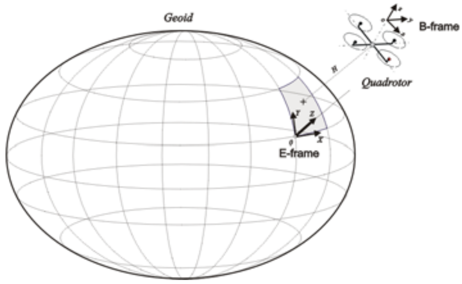

Figure 4
Earth- and Body-frame used for modeling of the quad-rotor system

$$s = [X\ Y\ Z\ \phi\ \theta\ \psi]^T \tag{1}$$

The rotation matrix between the E- and B-frames has the following form [3]:

$$R = \begin{bmatrix} c_\psi c_\theta & -s_\psi c_\phi + c_\psi s_\theta s_\phi & s_\psi s_\phi + c_\psi s_\theta c_\phi \\ s_\psi c_\theta & c_\psi c_\phi + s_\psi s_\theta s_\phi & -c_\psi s_\phi + s_\psi s_\theta c_\phi \\ -s_\theta & c_\theta s_\phi & c_\theta c_\phi \end{bmatrix} \tag{2}$$

The corresponding transfer matrix has the form:

$$T = \begin{bmatrix} 1 & s_\phi t_\theta & c_\phi t_\theta \\ 0 & c_\phi & -s_\phi \\ 0 & s_\phi / c_\theta & c_\phi / c_\theta \end{bmatrix} \tag{3}$$

In the previous two equations (and in the following) this notation has been adopted: $s_{(.)} = \sin(.)$, $c_{(.)} = \cos(.)$, $t_{(.)} = \tan(.)$. Now, the system Jacobian matrix, taking (2) and (3), can be written in the form:

$$J = \begin{bmatrix} R & 0_{3x3} \\ 0_{3x3} & T \end{bmatrix} \tag{4}$$

where 0_{3x3} is a zero-matrix. The generalized quad-rotor velocity in the B-frame has a form [3]:

$$v = \left[\dot{x}\ \dot{y}\ \dot{z}\ \dot{\phi}\ \dot{\theta}\ \dot{\psi}\right]^T \tag{5}$$

Finally, the kinematical model of the quad-rotor can be defined in the following way:

$$\dot{s} = J \cdot v \tag{6}$$

The dynamics of a generic 6 DOF rigid-body system takes into account the mass of the body *m* (kg) and its inertia matrix I ($Nm\ s^2$). Two assumptions have been done in this approach:

- The first one states that the origin of the body-fixed frame is coincident with the center of mass (COM) of the body. Otherwise, another point (COM) should be taken into account, which could make the body equations considerably more complicated without significantly improving model accuracy.
- The second one specifies that the axes of the B-frame coincide with the body principal axes of inertia. In this case the inertia matrix I is diagonal and, once again, the body equations become simpler.

The dynamic model of a quad-rotor can be defined in the following matrix form:

$$M_B\dot{v} + C_B(v)v - G_B = \Lambda \tag{7}$$

where M_B is the system Inertia matrix, C_B represents the matrix of Coriolis and centrifugal forces and G_B is the gravity matrix. The mentioned matrices have the known forms as presented in [3].

A generalized force vector Λ has the form [3]:

$$\Lambda = O_B(v)\Omega + E_B\Omega^2 \tag{8}$$

where:

$$O_B = J_{TP}\begin{bmatrix} 0 & 0 & 0 & 0 \\ 0 & 0 & 0 & 0 \\ 0 & 0 & 0 & 0 \\ \dot{\theta} & -\dot{\theta} & \dot{\theta} & -\dot{\theta} \\ -\dot{\phi} & \dot{\phi} & -\dot{\phi} & \dot{\phi} \\ 0 & 0 & 0 & 0 \end{bmatrix} \tag{9}$$

is the gyroscopic propeller matrix and J_{TP} is the total rotational moment of inertia around the propeller axis. The movement aerodynamic matrix has the form [3]:

$$E_B = \begin{bmatrix} 0 & 0 & 0 & 0 \\ 0 & 0 & 0 & 0 \\ b & b & b & b \\ 0 & -b \cdot l & 0 & b \cdot l \\ -b \cdot l & 0 & b \cdot l & 0 \\ -d & d & -d & d \end{bmatrix} \tag{10}$$

where b ($N\ s^2$) and d ($N\ m\ s^2$) are thrust and drag factors [3] and l (m) is the distance between the center of the quad-rotor and the center of the propeller. Equation (11) defines the overall propellers' speed (rad s^{-1}) and the propellers' speed vector (rad s^{-1}) used in equation (8).

$$\omega = -\omega_1 + \omega_2 - \omega_3 + \omega_4 \tag{11}$$

$$\Omega = \begin{bmatrix} \omega_1 & \omega_2 & \omega_3 & \omega_4 \end{bmatrix}^T \tag{12}$$

Equations (1)-(12) take into account the entire quad-rotor non-linear model including the most influential effects.

2.3 Control Strategy

In this section we present a control strategy to stabilize of the quad-rotor. Fig. 5 shows the block diagram of the quad-rotor control system.

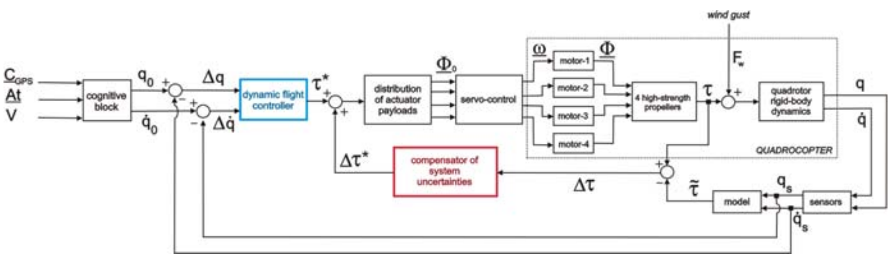

Figure 5

The block diagram of the quad-rotor control system

3 GPS Navigation of Quad-Rotor

The trajectory of the quad-rotor can be introduced by GPS coordinates (e.g. $\underline{P}_{GPS}(j)$) as shown in Fig. 6.

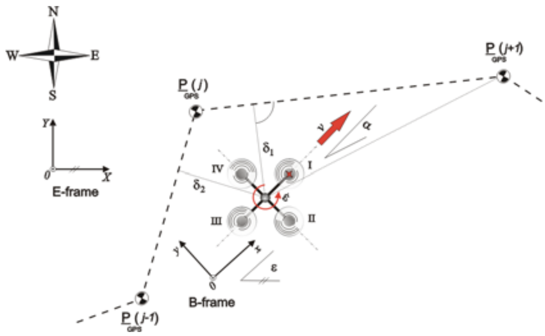

Figure 6
Quad-rotor localization and navigation with respect to the imposed GPS coordinates

The quad-rotor is requested to track the imposed trajectory between the particular points ($j = 1,...,n$) with satisfactory precision, keeping the desired attitude and height of flight. The quad-rotor checks for the current position (X and Y) by use of a GPS sensor and/or electronic compass. Also, the altitude is measured by a barometric sensor. An on-board microcontroller calculates the actual position deviation from the imposed trajectory given by successive GPS positions $\underline{P}_{GPS}(j)$. It localizes itself with respect to the nearest trajectory segment (by calculation of the distances δ_1 or δ_2). Using the gyroscope, the quad-rotor determines desired azimuth of flight α (Fig. 6) and keeps the desired direction of flight. The height of flight is also controlled to enable the performance of the imposed mission (task). One characteristic example of imposing quad-rotor trajectory by use of GPS coordinates is given in the next paragraph.

The corresponding Google Earth map is utilized to provide corresponding GPS coordinates of the quad-rotor trajectory as presented in Fig. 7.

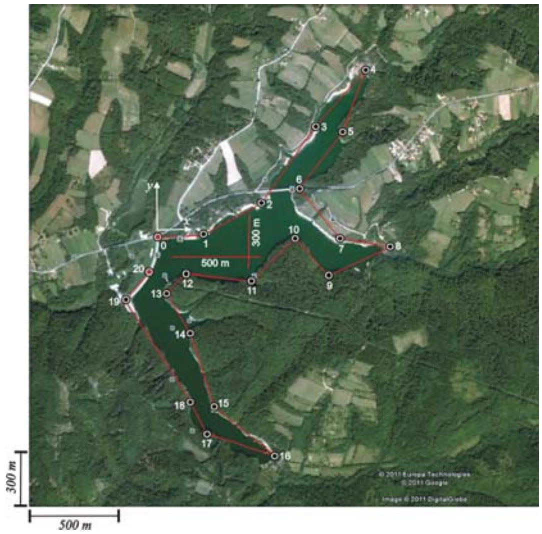

Figure 7
Google-Earth map of the Garaši lake used to define desired GPS trajectory of the quad-rotor aerial robot

GPS coordinates (longitude, latitude and altitude), defined in the map and given in the Fig. 8, are used to calculate quad-rotor trajectory in the E-frame.

	LONGITUDE			LATITUDE			ATTITUDE
point	degrees	minutes'	seconds"	degrees	minutes'	seconds"	feet
0	44	17	20.88	20	28	24.19	970
0'	44	17	20.88	20	28	24.19	970
1	44	17	21.44	20	28	36.04	963
2	44	17	27.11	20	28	50.67	964
3	44	17	40.87	20	29	4.07	970
4	44	17	51.45	20	29	17.09	968
5	44	17	39.87	20	29	11.14	987
6	44	17	29.61	20	29	0.2	980
7	44	17	20.63	20	29	10.35	970
8	44	17	19.05	20	29	23.15	991
9	44	17	14.02	20	29	7.53	1049
10	44	17	20.72	20	28	59.15	985
11	44	17	13.12	20	28	48.47	1045
12	44	17	14.54	20	28	31.86	983
13	44	17	11.05	20	28	26.98	987
14	44	17	3.83	20	28	32.98	970
15	44	16	50.71	20	28	39.13	1007
16	44	16	41.90	20	28	54.12	970
17	44	16	46.05	20	28	37.28	1036
18	44	16	53.58	20	28	31.58	1016
19	44	17	9.90	20	28	16.59	983
20	44	17	14.95	20	28	22.6	943
20'	44	17	14.95	20	28	22.6	943

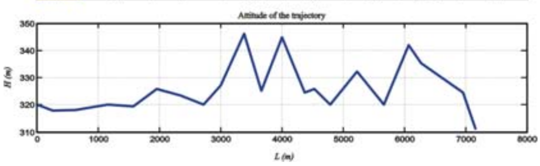

Figure 8
GPS coordinates acquired from the Google Earth map and used for the determination of the desired quad-rotor trajectory

Corresponding model of the trajectory given in E-frame is presented in Fig. 9.

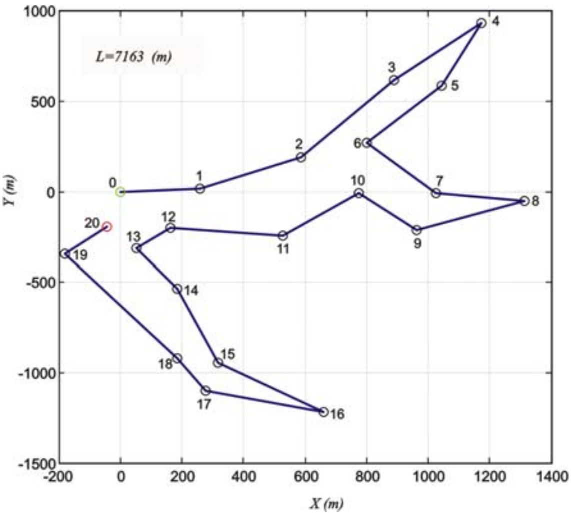

Figure 9
Multi-segment trajectory model of the quad-rotor determined in the E-frame

4 Simulation Example

Corresponding modeling and simulation software of rotorcraft aerial robots is developed in Matlab/Simulink. The open-loop simulation is performed and results are presented in the paper to verify model capabilities and system analysis. Aiming towards this goal, a quad-rotor flight is simulated by imposing corresponding particular propeller angular velocities presented in Fig. 10.

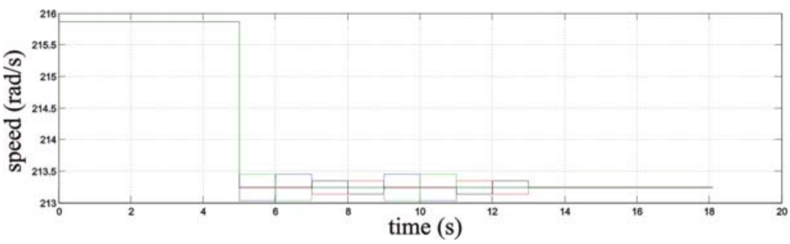

Figure 10
Example of the imposed propeller angular velocities that enable desired movements of quad-rotor

The imposed movements include several flight phases: (i) throttle movements in the vertical direction, (ii) counter-clockwise roll movements, (iii) tilt movement about the pitch axis, and (iv) hovering with a constant propeller speed. One sequence of the simulation test-flight is presented by the 3D-plot in Fig. 11.

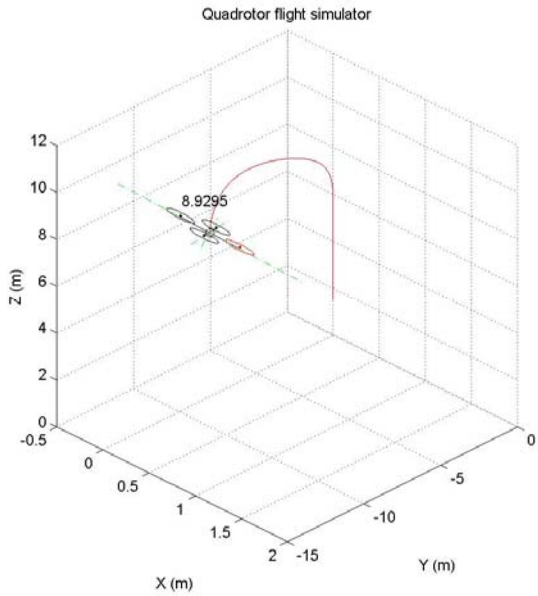

Figure 11
3D-plot of the quad-rotor simulation flight

Corresponding roll and pitch movements, due to the imposed variation of rotors' speeds, are presented in Fig. 12.

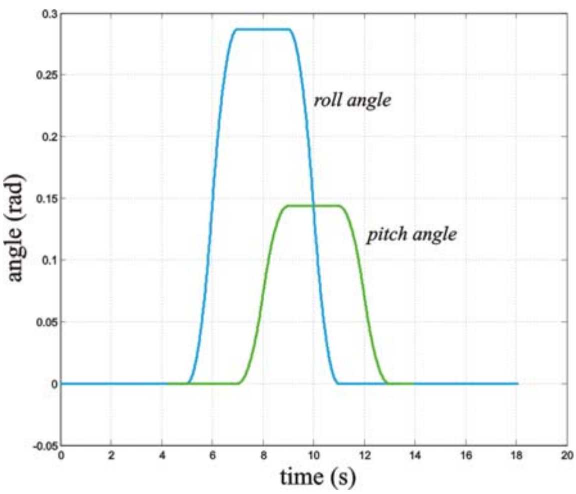

Figure 12
Roll and pitch movements due to the imposed propeller rotations given in Fig. 9

The quad-rotor trajectory projection in the X-Y plane is given in Fig. 13. Changing of the quad-rotor height during flight is given in Fig. 14.

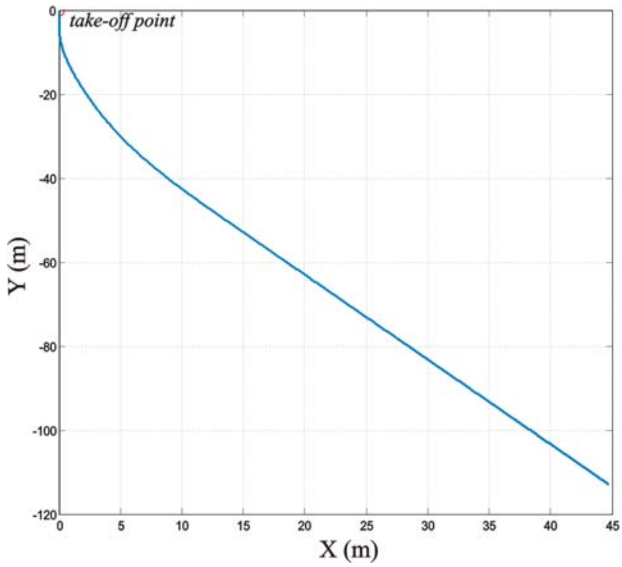

Figure 13
Quad-rotor movements in X- and Y-direction

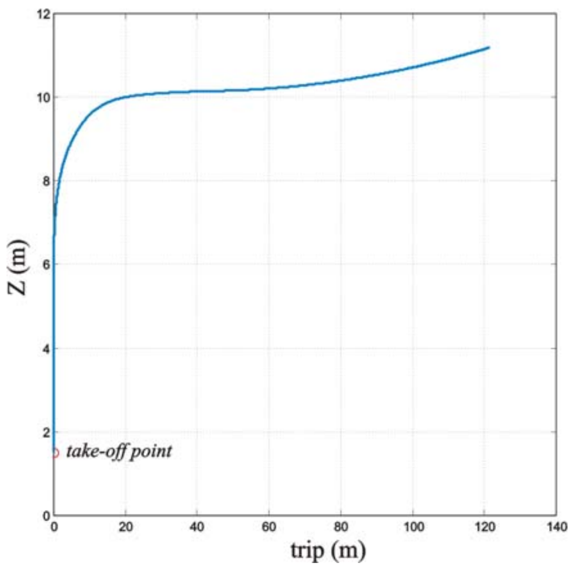

Figure 14
Quad-rotor movements in Z-direction

Conclusions

The paper considers the modeling and simulation of an autonomous quad-rotor microcopter in a virtual outdoor scenario. The main contribution of this paper focuses on the development of a flight simulator to provide an advanced R/D tool suitable for control design and model evaluation of a quad-rotor system to be used for control algorithm development and verification before working with real experimental systems. The main aspects of modeling of rotorcraft kinematics and rigid body dynamics, spatial system localization and navigation in virtual outdoor scenario are considered in the paper. Finally, several basic maneuvers are investigated and simulated in the paper to verify the simulation software capabilities and engineering capabilities.

Acknowledgement

This work was supported by the innovation project 'Research and Development of Ambientally Intelligent Service Robots', TR-35003, 2011-2014, funded by the Ministry of Science of the Republic Serbia and partially supported by the TÁMOP-4.2.2/08/1/2008-0008 program of the Hungarian National Development Agency.

References

[1] C. Lebres, V. Santos, N. M. Fonseca Ferreira and J. A. Tenreiro Machado: Application of Fractional Controllers for Quad Rotor, Nonlinear Science and Complexity, Part 6, DOI: 10.1007/978-90-481-9884-9_35, Springer, 2011, pp. 303-309

[2] J. Coelho, R. Neto, C. Lebres, V. Santos: Application of Fractional Algorithms in Control of a Quad Rotor Flight, Proceedings of the 2nd Conference on Nonlinear Scienceand Complexity, Porto, Portugal, July 28-31, 2008, pp. 1-12

[3] Tommaso Bresciani, Modelling, Identification and Control of a Quadrotor Helicopter, Department of Automatic Control, Lund University, ISSN 0280-5316, ISRN LUTFD2/TFRT/5823.SE, October 2008

[4] B. Siciliano and O. Khatib, Eds., Handbook of Robotics, Springer, ISBN: 978-3-540-23957-4, 2008, pp. 391-410

[5] Barnes W. and McCormick, W., Aerodynamics Aeronautics and Flight Mechanics. New York: Wiley, 1995

[6] Gordon Leishman, J., Principles of Helicopter Aerodynamics, Second Edition, Cambridge University Press, 1995

[7] Etkin, B. and Reid L. R., Dynamics of Flight- Stability and Control. John Wiley & Sons. New York, 1996

[8] Castillo, P. Dzul, A. Lozano, R. Stabilization of a Mini Rotorcraft Having Four Rotors, Control Systems Magazine, Vol. 25, No. 6, pp. 45-55, December 2005.Authors: Title

[9] Aircraft X650 Quad-rotor, http://www.infmetry.com/coolstuff/xaircraft-x650-quadcopterquadrotor/

[10] Aleksandar Rodic, Gyula Mester, "Modeling and Simulation of Quad-Rotor Dynamics and Spatial Navigation", Proceedings of the SISY 2011, 9th IEEE International Symposium on Intelligent Systems and Informatics, pp 23-28, ISBN: 978-1-4577-1973-8, Subotica, Serbia, September 8-10, 2011

[11] Ján Lábun, František Adamčík, Ján Pil'a, Ladislav Madarász: Effect of the Measured Pulses Count on the Methodical Error of the Air Radio Altimeter, in Acta Polytechnica Hungarica, Vol. 7, No. 1, 2010, pp. 41-49